Antimicrobial Agents and Chemotherapy

Mutations in the Pseudomonas aeruginosa Needle Protein Gene *pscF* Confer Resistance to Phenoxyacetamide Inhibitors of the Type III Secretion System

Nicholas O. Bowlin, John D. Williams, Claire A. Knoten, Matthew C. Torhan, Tommy F. Tashjian, Bing Li, Daniel Aiello, Joan Mecsas, Alan R. Hauser, Norton P. Peet, Terry L. Bowlin and Donald T. Moir

Antimicrob. Agents Chemother. **2014, 58(4):2211. DOI: 10.1128/AAC.02795-13.**
Published Ahead of Print 27 January 2014.

AAC Journals.ASM.org

Mutations in the *Pseudomonas aeruginosa* Needle Protein Gene *pscF* Confer Resistance to Phenoxyacetamide Inhibitors of the Type III Secretion System

Nicholas O. Bowlin,[a] John D. Williams,[a] Claire A. Knoten,[b] Matthew C. Torhan,[a] Tommy F. Tashjian,[a] Bing Li,[a] Daniel Aiello,[a] Joan Mecsas,[c] Alan R. Hauser,[b] Norton P. Peet,[a] Terry L. Bowlin,[a] Donald T. Moir[a]

Microbiotix, Inc., Worcester, Massachusetts, USA[a]; Departments of Microbiology/Immunology and Medicine, Northwestern University, Chicago, Illinois, USA[b]; Department of Molecular Biology and Microbiology, Tufts University School of Medicine, Boston, Massachusetts, USA[c]

The type III secretion system (T3SS) is a clinically important virulence mechanism in *Pseudomonas aeruginosa* that secretes and translocates effector toxins into host cells, impeding the host's rapid innate immune response to infection. Inhibitors of T3SS may be useful as prophylactic or adjunctive therapeutic agents to augment the activity of antibiotics in *P. aeruginosa* infections, such as pneumonia and bacteremia. One such inhibitor, the phenoxyacetamide MBX 1641, exhibits very responsive structure-activity relationships, including striking stereoselectivity, in its inhibition of *P. aeruginosa* T3SS. These features suggest interaction with a specific, but unknown, protein target. Here, we identify the apparent molecular target by isolating inhibitor-resistant mutants and mapping the mutation sites by deep sequencing. Selection and sequencing of four independent mutants resistant to the phenoxyacetamide inhibitor MBX 2359 identified the T3SS gene *pscF*, encoding the needle apparatus, as the only locus of mutations common to all four strains. Transfer of the wild-type and mutated alleles of *pscF*, together with its chaperone and co-chaperone genes *pscE* and *pscG*, to a Δ*pscF P. aeruginosa* strain demonstrated that each of the single-codon mutations in *pscF* is necessary and sufficient to provide secretion and translocation that is resistant to a variety of phenoxyacetamide inhibitor analogs but not to T3SS inhibitors with different chemical scaffolds. These results implicate the PscF needle protein as an apparent new molecular target for T3SS inhibitor discovery and suggest that three other chemically distinct T3SS inhibitors interact with one or more different targets or a different region of PscF.

Type III secretion systems (T3SSs) are complex nanomachines made by many Gram-negative bacterial species for the purpose of injecting effector proteins into eukaryotic cells (1, 2). The T3SS of the opportunistic pathogen *Pseudomonas aeruginosa*, which consists of nearly 40 gene products, translocates effector toxins into host macrophages and neutrophils, reducing the host's ability to respond to infection (3, 4). The T3SS is not essential for *P. aeruginosa* viability *in vitro* but is crucial for the establishment and dissemination of *P. aeruginosa* infections. This is evident by the severely depleted bacterial burdens of T3SS mutant strains in animal models of acute pneumonia (5, 6) and by the poorer clinical outcomes associated with T3SS-competent *P. aeruginosa* strains in patients with ventilator-associated pneumonia (VAP) and bacteremia (7–11). These results validate the *P. aeruginosa* T3SS as an important target for therapeutic and/or prophylactic intervention. Indeed, several inhibitors of *P. aeruginosa* T3SS have been described, both small molecules (12–16) and monoclonal antibodies (17, 18). The most advanced of these agents, KB001, is an anti-PcrV monoclonal antibody currently in clinical studies (19, 20). PcrV is a needle-tip protein that mediates the folding and insertion of PopB/PopD into host membranes as part of the translocation channel, and to date, it has been the only defined structural protein target of a T3SS inhibitor (21). We now describe experiments to identify the molecular target of a series of phenoxyacetamide small-molecule inhibitors previously shown to exhibit very responsive structure-activity relationships (SAR), including an extremely high degree of stereoselectivity, in blocking the *P. aeruginosa* T3SS (15). Results implicate the needle protein PscF as a new T3SS target that is vulnerable to chemical intervention.

MATERIALS AND METHODS

Strains, plasmids, and growth media. Bacterial strains and plasmids used for assays are described in Table 1. All *P. aeruginosa* strains were derivatives of PAO1 (22) or PAK (23). *Escherichia coli* TOP10 (Invitrogen), *E. coli* DB3.1 (Gateway host; Invitrogen), *E. coli* SM10 (24), and *E. coli* S17-1 (ATCC 47055) were used as hosts for molecular cloning. Vogel-Bonner minimal medium (VBMM) was made as described previously (24). Luria-Bertani (LB) medium (liquid and agar) was purchased from Difco. LB was supplemented with gentamicin (LBG) at the indicated levels with 0.1 mM isopropyl-β-D-thiogalactopyranoside (IPTG) and 3 mM EGTA, as noted in each experiment.

PCR and primers. Synthetic oligonucleotide primers (from Operon, Inc.) were designed using the published genome sequence for *P. aeruginosa* (25) and web-based PRIMER3 (Whitehead Institute) (Table 2). Primers were used at 10 μM in PCR amplifications with PhusionGC polymerase (New England BioLabs) for *P. aeruginosa* chromosomal DNA templates.

Construction of a mutant selection strain. A *P. aeruginosa* strain was engineered to enable selection for mutants that are resistant to T3SS inhibitors. First, a transcriptional fusion of the gentamicin resistance (Gm^r) gene *aacC1* to the T3SS effector gene *exoT* promoter was integrated into the PAO1 efflux-deficient derivative PA0397 (26). Specifically, the pGSV3-*exoT-luxCDABE* plasmid in strain MDM850 (Table 1) (15) was

Received 26 December 2013 Returned for modification 17 January 2014
Accepted 23 January 2014
Published ahead of print 27 January 2014
Address correspondence to Donald T. Moir, dmoir@microbiotix.com.

doi:10.1128/AAC.02795-13

TABLE 1 Strains and plasmids

Strain	Description	Reference or source
E. coli		
MDM468	TOP10/pUCP24GW-lacI^{Q}PO	32
MDM850	SM10/pGSV3-*exoT-luxCDABE* Sp^{r}	15
MDM1385	SM10/pGSV3-*exoT-aacC1* Sp^{r}	This study
MDM1696	S17.1/miniCTX*exoS*(E379A/E381A)-*blaM*	This study
P. aeruginosa		
MDM973	PAK/pUCP24GW-*lacI^{Q}PO-exoT-luxCDABE*	15
PA0397	PAO1 Δ(*mexAB-oprM*) *nfxB* Δ(*mexCD-oprJ*) Δ(*mexEF-oprN*) Δ(*mexJKL*) Δ(*mexXY*) Δ*opmH362*	26
MDM1542	PAO397::pGSV3-Sp^{r}-*exoT*^{o}-*aacC1*	This study
MDM1710	MDM1542::miniCTX*exoS*(E379A/E381A)-*blaM*	This study
MDM1739	MDM1710 MBX-2359^{r} [*pscF*(G223T; R75C)]	This study
MDM1749	MDM1710 MBX-2359^{r} [*pscF*(G224A; R75H)]	This study
MDM1750	MDM1710 MBX-2359^{r} [*pscF*(G184A; V62I)]	This study
MDM1770	MDM1710 MBX-2359^{r} [*pscF*(G239A, G80D)]	This study
MDM1838	PAO1 Δ*pscF*::miniCTX-*exoS*(E379A/E381A)-*blaM*	This study
MDM1912	MDM1838/pUCP24GWGm-*lacI^{Q}PO-pscE-pscF*(WT)-*pscG*	This study
MDM1886	MDM1838/pUCP24GWGm-*lacI^{Q}PO-pscE-pscF*(R75H)-*pscG*	This study
MDM1967	MDM1838/pUCP24GWGm-*lacI^{Q}PO-pscE-pscF*(V62I)-*pscG*	This study
MDM1938	MDM1838/pUCP24GWGm-*lacI^{Q}PO-pscE-pscF*(R75C)-*pscG*	This study
MDM1940	MDM1838/pUCP24GWGm-*lacI^{Q}PO-pscE-pscF*(G80D)-*pscG*	This study

modified by replacing its gentamicin resistance marker with a spectinomycin resistance marker as described previously (27) and by replacing the *luxCDABE* fragment with *aacC1*. This was accomplished by digestion with NotI restriction endonuclease to release *luxCDABE* followed by ligation of a NotI-ended *aacC1* fragment amplified from pUCP24 DNA by PCR using primers aacC1+Not-F and aacC1+Not-R (Table 2). The resulting plasmid, pGSV3-Sp^{r}-*exoT-aacC1*, was introduced into PA0397 by conjugation, and single-crossover integrants at *exoT* were confirmed by PCR with primers exoT-out-F and aacC1+Not-R (Table 2). The resulting strain MDM1542 (Table 1) exhibits Gm^{r} that is dependent on induction of T3SS and lost in the presence of T3SS inhibitors. A single copy of a gene encoding full-length ExoS (lacking adenosine diphosphate ribosyltransferase [ADPRT] activity due to two mutations, E379A/E381A) fused to TEM1 β-lactamase (BLA) on miniCTX1 (28) was constructed essentially as described previously for miniCTXexoU-BLA (29). First, the stop codon was removed from *exoS* using the primers exoSdeltastopF and exoSdeltastopR (Table 2). A fragment of TEM-1 β-lactamase (bla) was amplified from pBR322 with 3′ AgeI and 5′ AgeI sites using primers blaCAgeUp and blaCAgeDwn. These fragments were cloned into miniCTX to generate miniCTXexoS-BLA. Site-directed mutagenesis was then performed using the following primers to generate the ADPRT mutations: E379A/E381A-forward and E379A/E381A-reverse. The resulting miniCTXexoS-BLA was integrated into the chromosome of MDM1542 to yield selection strain MDM1710 (Table 1).

TABLE 2 Primers

No.	Name	Sequence[a]
1	aacC1+Not-F	ataagaatgcggccgcccgcaaaatggatgttacgcagcagcaacga
2	aacC1+Not-R	acggtcagcggccgccgaattgttaggtggcggta
3	exoT-out-F	tagggaaagtccgctgtttt
4	exoSdeltastopF	ggccttgatctggccggaccggtcgtaaa
5	exoSdeltastopR	cgtctttcttttacgaccggtccggccagat
6	blaCAgeUp	aaaaccggtacacccagaaacgct
7	blaCAgeDwn	aaaaccggtattaccaatgcttaatcagtga
8	E379A/E381A-forward	cgaactacaagaatgcaaaagcgatttctctataacaaag
9	E379A/E381A-reverse	ttgttatagagaatcgcttttgcattcttgtagttcgat
10	pscF-Up-F+GWL	TACAAAAAAGCAGGCTgctcgtcgaaccctggtc
11	pscF-Up-R	atcttctgcaggatgccttgcgcCATgcttagtcctctgt
12	pscF-Dwn-F	acagaggactaagcATGgcgcaaggcatcctgcagaagat
13	pscF-Dwn-R+GWR	TACAAGAAAGCTGGGTacagctccatctgcaactcc
14	pscF-Out-F	gagttttcccgagcgtttc
15	pscF-Out-R	tgggtcttcatcagggtttc
16	GW-Universal-attB1	ggggacaagtttgtacaaaaaagcaggct
17	GW-Universal-attB2	ggggaccactttgtacaagaaagctgggt
18	pscEFG-F+attB1	ggggacaagtttgtacaaaaaagcaggctgaggtgctccATGatgacag
19	pscEFG-R+attB2	ggggaccactttgtacaagaaagctgggtgacggatagacggcgaatc

[a] Partial *attB1* and *attB2* tails are in uppercase letters, as are the *pscF* start and stop codons.

Selection for phenoxyacetamide-resistant mutants. Selection strain MDM1710 was subjected to mutagenesis with ethyl methanesulfonate essentially as previously described (30) to a 1% auxotrophy rate, as determined by replica plating on rich (LB) and minimal (VBMM) media. Inhibitor-resistant mutants of MDM1710 were selected from a total of about 6×10^{6} mutagenized cells for growth on agar medium in the presence of 1 mM EGTA (to induce T3SS), 16 μg/ml Gm, and 25 μM T3SS inhibitor MBX 2359. Gentamicin-resistant colonies were transferred to nonselective medium, grown, and replica plated onto three VBMM plates with the following supplements: 16 μg/ml Gm (plate a); 1 mM EGTA, 16 μg/ml Gm (plate b); and 1 mM EGTA, 16 μg/ml Gm, 25 μM MBX 2359 (plate c). Mutants that were confirmed to exhibit gentamicin resistance, which was dependent on the addition of EGTA (i.e., growth on plate b but not on plate a) but independent of the addition of MBX 2359 (i.e., growth on both plates b and c), were evaluated for T3SS-mediated secretion of the ExoS-BLA fusion protein in the presence of MBX 2359 by colorimetric assay (below). Mutant strains exhibiting significantly increased 50% inhibitory concentrations (IC_{50}s) for MBX 2359 inhibition were characterized further.

Mapping mutations to resistance by sequencing. Genomic DNA was prepared from three inhibitor-resistant mutants as well as from the wild-type parent MDM1710 (TIP20 kit; Qiagen) and analyzed by Illumina next-generation sequencing for single-nucleotide polymorphisms (SNPs) between the parent and each mutant (SeqWright, Inc.).

Construction of a *pscF* deletion strain. Strain MDM1838 (Table 1), an in-frame, markerless deletion of the *pscF* gene leaving 2 amino-terminal and 7 carboxy-terminal codons, was generated from *P. aeruginosa* strain PAO1 containing an integrated miniCTX-*exoS*(E379A/E381A)-*blaM* construct by standard Gateway and PCR splicing by overlap exten-

sion technology and confirmed by sequencing as described previously (31). Primers 10 to 17 were used (Table 2; partial *attB1* and *attB2* tails are in uppercase letters, as are the *pscF* start and stop codons).

Complementation of *pscF* deletion strains. The three-gene cluster *pscE-pscF-pscG* was amplified by PCR from wild-type and mutant strains using primers pscEFG-F+attB1 and pscEFG-R+attB2 (Table 2), cloned into pDONR221 by Gateway cloning, sequenced to confirm that the appropriate *pscF* mutations were present, and moved into the pUPC24GW-lacI^{Q}PO recipient vector (Table 1) for expression from the *lac* promoter (32). Resulting pUPC24GW-lacI^{Q}PO plasmids carrying *pscF* mutant alleles were transferred by electroporation (33) to Δ*pscF P. aeruginosa* cells to confirm their role in inhibitor resistance. Cells were grown in the presence of 0.1 mM isopropyl-β-D-thiogalactopyranoside (IPTG) for expression of *pscF* alleles.

Colorimetric detection of T3SS-mediated secretion of ExoS-BLA. Secretion of ExoS-BLA fusion protein into culture medium was detected by measuring the hydrolysis of the chromogenic β-lactamase substrate nitrocefin (Acme Bioscience, Inc., Palo Alto, CA) by A_{490} in clear 96-well microplates as described previously (15).

Immunoblotting detection of T3SS-mediated effector secretion into culture broth. Overnight cultures of MDM1710 were grown in LB medium (5 ml in a 14-ml tube) at 37°C at ≥250 rpm. Overnight cultures (50 μl, 1:100 dilution) were used to inoculate 5 ml of LB plus 5 mM EGTA. MBX 2359 was added at the concentrations indicated. Cultures were grown for 4 h at 37°C at ≥250 rpm. Supernatant from each culture, normalized to cell number, was precipitated with trichloroacetic acid and resuspended in 40 μl of 1× sample buffer, and 30 μl from each sample was applied to an SDS-PAGE gel. The samples were electrophoresed at 150 V for an hour using Tris-glycine gels in 1× Tris-glycine-SDS buffer. The proteins were then transferred to a nitrocellulose membrane (Bio-Rad) by wet transfer using 1× transfer buffer (1× Tris-glycine, 10% methanol) at 100 V for 1 h. Blots were incubated with primary antibody against ExoS (34), followed by a proprietary goat anti-rabbit secondary antibody (Li-Cor). Blots were imaged using the LiCor imager, channel 700, for 2 min. All edits were done to entire images. A LiCor 928-40000 protein ladder was used to estimate protein molecular weights.

T3SS-mediated translocation assays. The translocation of ExoS-BLA was assayed as follows. J774 cells seeded in 96-well black tissue culture-treated plates (Costar, Corning Inc.) were infected at a multiplicity of infection (MOI) of 10, centrifuged at 1,000 rpm for 5 min, and then incubated at 37°C for 90 min. The cells were loaded with a final concentration of 1.2 μM hydroxycoumarin cephalosporin fluorescein-acetoxymethyl ester (CCF2-AM) (Invitrogen) and incubated for 1 h at room temperature. The plates were analyzed in a bottom-read SynergyH1 (BioTek) fluorescence plate reader. Excitation was set at 410 nm; emissions at 460 nm and 530 nm were recorded. The blue/green fluorescence ratio was calculated by the formula $(RFU_{460\ nm} - RFU_{460\ nm,\ background})/(RFU_{530\ nm} - RFU_{530\ nm,\ background})$, where RFU is relative fluorescence units and background fluorescence is fluorescence emission from cells that were infected but not loaded with CCF2-AM.

Chemistry. Phenoxyacetamide MBX 1641 was prepared as described previously (15). The phenoxyacetamide analogs MBX 2614 and MBX 2727 were prepared in a similar manner from the commercially available acid 2-(2,4-dichlorophenoxy)propanoic acid and the corresponding amine or hydrazine using the peptide coupling reagent HATU. MBX 2164 was synthesized by HATU-promoted peptide coupling of 2-(2,4-dichlorophenylthio)propanoic acid. 2-(3,5-Dichloropyridy-2-oxy)propanoic acid was synthesized via a Mitsunobu reaction of 3,5-dichloro-2-pyridone and ethyl lactate followed by saponification and coupled to 5-aminomethylbenzothiophene to provide MBX 2359. The (*R*)- and (*S*)-stereoisomers of MBX 2359, denoted as MBX 2401 and MBX 2402, respectively, were separated from the racemate MBX 2359 by using chiral high-performance liquid chromatography (HPLC). Two nonphenoxyacetamide T3SS inhibitors, CBG-5376648 and CBG-6594330, were purchased from ChemBridge Corp. (San Diego, CA), and a third one, INP0007, was synthesized as previously described (35).

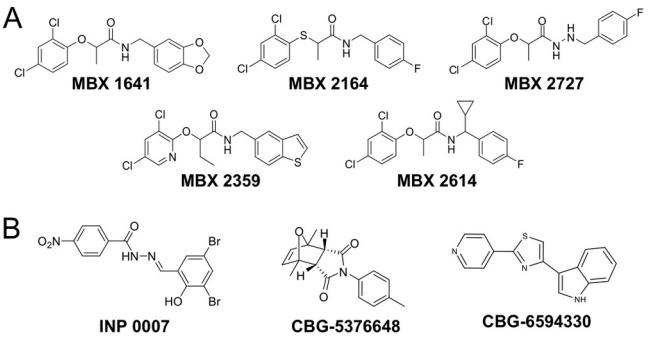

FIG 1 Structures of small-molecule inhibitors of *P. aeruginosa* T3SS used in this study. (A) Five analogs of the phenoxyacetamide series, including MBX 2359, which was used for selection of resistant mutants. (B) Representatives of three published nonphenoxyacetamide scaffolds.

Homology model of polymerized PscF. A homology model of PscF assembled in a needle was generated using a comparative modeling approach, which was implemented with the Schrödinger computational software (Schrödinger, LLC). The structure of the *Salmonella enterica* serovar Typhimurium T3SS needle composed of assembled PrgI subunits, generated by cryoelectron microscopy and solid-state nuclear magnetic resonance (NMR) (36), was used as the template (PDB entry 2LPZ). A total of 29 PscF subunits were constructed in the homology model.

RESULTS

A more potent phenoxyacetamide analog for resistance selection. The previously reported selectivity of T3SS inhibition and responsive SAR, including pronounced stereoselectivity of inhibition, suggested that the phenoxyacetamide inhibitors specifically target one or more components of the T3SS (15). To test this hypothesis, we undertook an identification of the phenoxyacetamide target by isolating and characterizing suppressor mutants. First, we developed a more potent optimized analog of the original phenoxyacetamide T3SS inhibitor to facilitate resistance selection. Based on the SAR gleaned from about 300 analogs (15) (J. D. Williams, unpublished data), the pyridyloxy-acetamide compound MBX 2359 (Fig. 1) was synthesized. This analog is approximately 8-fold more potent than the original screening hit MBX 1641 (IC_{50}, ~15 μM) for inhibition of T3SS-mediated secretion and retains the pronounced stereoselectivity (Fig. 2). Specifically, the (*R*)-isomer MBX 2401 (IC_{50}, ~1.2 μM) is about twice as potent as the racemate MBX 2359 (IC_{50}, ~2.5 μM), and the (*S*)-isomer MBX 2402 is inactive at concentrations of up to 50 μM (Fig. 2). Since it is more potent than the previously published phenoxyacetamide inhibitor (MBX 1641) and is more feasible to prepare on a moderate scale than is the (*R*)-isomer (MBX 2401; see Materials and Methods), the racemate MBX 2359 was used in agar medium to select for mutant *P. aeruginosa* clones whose T3SS exhibited significant resistance to the analog as described below.

Mutations conferring resistance to the T3SS inhibitor MBX 2359 reside in the *pscF* gene. Identifying bacterial mutations that provide resistance to small-molecule antibacterial compounds is a commonly used approach to identify the likely target of inhibitors. However, application of this approach to inhibitors of T3SS is complicated by the fact that this virulence factor is not required for growth of *P. aeruginosa* cells in culture. Accordingly, we engineered a strain of *P. aeruginosa* to enable selection for resistant

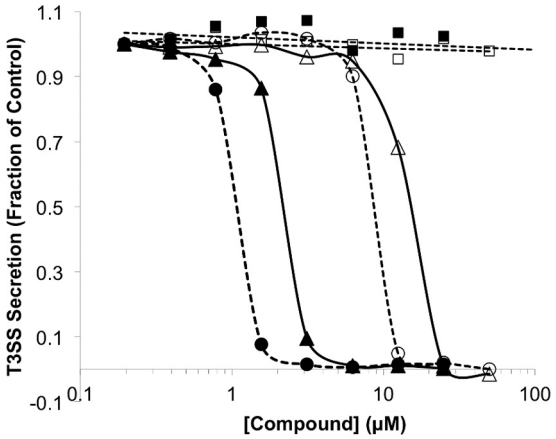

FIG 2 Stereoselective inhibition of T3SS-mediated secretion by phenoxyacetamide inhibitors. Inhibition of T3SS-mediated secretion of ExoS-BLA from *P. aeruginosa* strain MDM973 is shown. Inhibitors include the original screening hit, racemate MBX 1641 (Δ), its (*R*)-isomer, MBX 1684 (O), its (*S*)-isomer, MBX 1686 (□), and an analog optimized for potency, the racemate MBX 2359 (▲), together with its (*R*)-isomer MBX 2401 (●) and (*S*)-isomer MBX 2402 (■). The fraction of secretion of ExoS-BLA into culture medium with respect to the control (uninhibited secretion), as measured by the change in absorbance at 490 nm per min resulting from the cleavage of nitrocefin (ΔA490/min), is plotted versus the concentration of compound added.

mutants. Our goal was to generate a strain that required ongoing type III secretion for viability. Addition of the phenoxyacetamide type III secretion inhibitor would then result in bacterial death, except in the presence of mutations that conferred resistance to the inhibitor. To construct such a strain (designated MDM1710), we took advantage of the previously described tight coupling of type III secretory activity with T3SS transcription (37, 38). The gentamicin resistance element *aacC1* was placed under the control of the T3SS-regulated *exoT* promoter, resulting in a *P. aeruginosa* strain that was resistant to gentamicin when type III secretion was induced by growth in low-calcium medium (e.g., addition of EGTA) but sensitive to gentamicin when type III secretion was blocked by addition of an inhibitor. The screening strain was also engineered to contain a chromosomally integrated copy of a reporter fusion protein gene consisting of the effector protein ExoS tagged with β-lactamase (designated ExoS-BLA) to enable convenient direct measurements of T3SS-mediated secretion.

To identify the target of MBX 2359 by mapping mutations to resistance, we selected gentamicin-resistant clones of ethyl methanesulfonate-mutagenized MDM1710 in the presence of both EGTA and MBX 2359. However, most of the resulting clones appeared to meet the selection by breaking the link between type III secretory activity and transcription and, consequently, constitutively expressing *accC1* rather than by escaping inhibition of secretion by MBX 2359. To discriminate between such regulatory mutants and true T3SS secretion-resistant mutants, the selected gentamicin-resistant clones were evaluated further in a screen for those that retained EGTA-dependent gentamicin resistance (i.e., gentamicin resistant in the presence of EGTA but gentamicin susceptible in the absence of EGTA). Clones that retained EGTA dependence were then assayed directly for ongoing type III secretion in the presence of inhibitor. This was accomplished by measuring hydrolysis of extracellular nitrocefin in the presence of bacteria secreting ExoS-BLA.

Four mutants with pronounced resistance of ExoS-BLA secretion to MBX 2359 were identified from about 1,200 gentamicin-resistant colonies selected. The MBX 2359 IC_{50}s shifted from

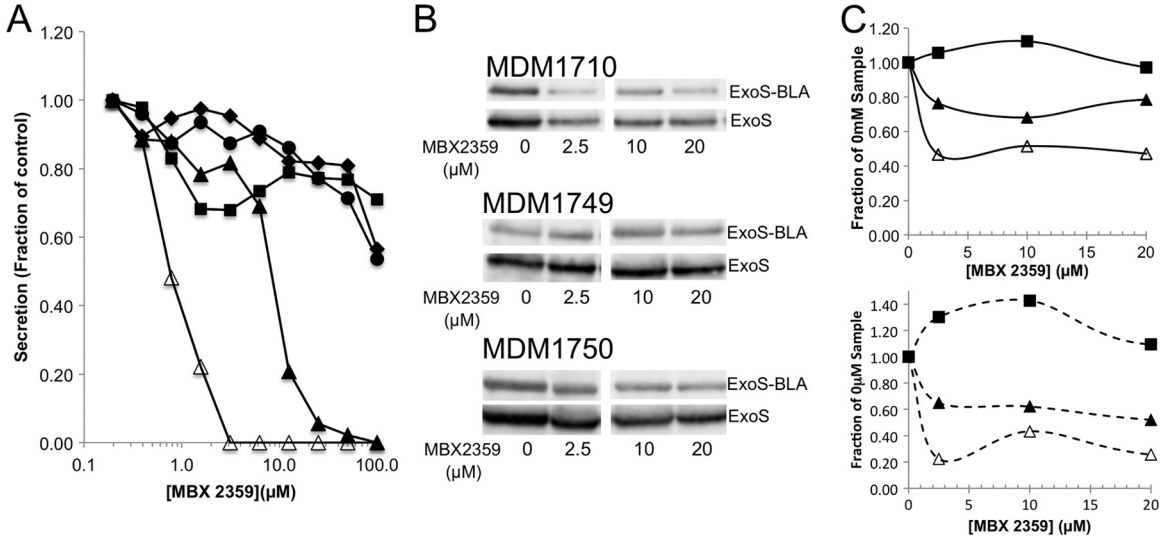

FIG 3 T3SS-mediated secretion by selected mutants is resistant to inhibition by MBX 2359. (A) Concentration dependence of MBX 2359 inhibition of T3SS-mediated secretion of ExoS-BLA by the *P. aeruginosa* screening strain MDM1710 (△) and four selected mutants, MDM1739 [PscF(R75C)] (●), MDM1749 [PscF(R75H)] (■), MDM1750 (PscF(V62I)] (▲), and MDM1770 [PscF(G80D)] (◆). Secretion was measured by the rate of hydrolysis of nitrocefin by ExoS-BLA. Results are plotted as a fraction of that of the uninhibited control versus the concentration of T3SS inhibitor MBX 2359 added. (B) Inhibition by MBX 2359 of T3SS-mediated secretion of native effector ExoS and ExoS-BLA fusion proteins into the culture medium was measured by immunoblot analysis. Supernatants (normalized to cell number) of the screening strain MDM1710, the highly resistant mutant MDM1749 [PscF(R75H)], and the moderately resistant mutant MDM1750 [PscF(V62I)] were analyzed. Detection was by primary anti-ExoS antibody and LiCor goat anti-rabbit as the secondary antibody. Blots were imaged using the LiCor imager. (C) Image-Studio (LiCor) was used to perform densitometry on each band. Densities were normalized to the no-inhibitor value and are shown graphically for MDM1710 (△), MDM1749 [PscF(R75H)] (■), and MDM1750 [PscF(V62I)] (▲) for ExoS (upper) and ExoS-BLA (lower).

TABLE 3 Change in potency of inhibition of T3SS-mediated secretion or translocation by *P. aeruginosa* cells containing wild-type or mutant *pscF* alleles[a]

Inhibitor and IC_{50} measured	IC_{50} (μM)					Fold shift			
	WT	V62I	R75C	R75H	G80D	V62I	R75C	R75H	G80D
Secretion									
MBX 1641	5.2	18	>100	>100	>100	3.5	>19	>19	>19
MBX 2359	1.1	10	70	>100	80	9.1	64	>90	72
MBX 2164	4	18	>100	>100	>100	4.5	>25	>25	>25
MBX 2614	3.6	10	80	>100	100	2.8	22	>27	28
MBX 2727	3.9	15	100	>100	100	3.8	26	>25	26
INP-0007	0.8	0.9	0.7	1	1.3	1.1	0.9	1.3	1.6
CBG-5376648	5	6	6	7	8	1.2	1.2	1.4	1.6
CBG-6594330	65	40	75	50	40	0.6	1.2	0.8	0.6
Translocation									
MBX 2359	10	20	>100	>100	>100	2.0	>10	>10	>10

[a] Strains used for each *pscF* allele were MDM1912 (WT), MDM1967 (V62I), MDM1938 (R75C), MDM1886 (R75H), and MDM1940 (G80D).

about 1.5 μM for the parent to >100 μM for three mutants and to 10 μM for the fourth mutant (Fig. 3A). Similar relative shifts in susceptibility to MBX 2359 were observed when secretion of native effector toxin ExoS and ExoS-BLA were measured directly by immunoblotting of culture medium from *P. aeruginosa* wild-type and mutant cells induced for T3SS and treated with inhibitor (Fig. 3B and C), although results were more variable and accompanied by a high background of secreted ExoS and ExoS-BLA. Genomic DNA was prepared from three of the mutants (MDM1739, MDM1749, and MDM1750) and the parent strain MDM1710 and subjected to Illumina sequencing to identify single-nucleotide polymorphisms (SNPs) between the mutants and parent. All three mutant strains harbored codon-altering SNPs in the same T3SS structural gene, *pscF*. Two mutant strains (MDM1739 and MDM1749) contained different changes in the same codon, G223T and G224A, altering the Arg75 codon to two different codons, Cys and His, respectively, and the third mutant strain (MDM1750) altered the nearby Val62 codon to Ile (G184A). No other single gene contained codon-altering SNPs in all three mutant strains compared to the wild-type parent. Direct sequencing of the *pscF* gene from the fourth mutant (MDM1770) revealed an alteration (G239A) of the Gly80 codon to an Asp codon. These results suggest that the PscF protein, which forms the T3SS needle apparatus of *P. aeruginosa*, is the target of MBX 2359.

Mutations in *pscF* are necessary and sufficient to confer inhibitor resistance to T3SS-mediated secretion and translocation. Since the selection strain had been subjected to chemical mutagenesis prior to selection, mutant *pscF* alleles were generated in a previously unmutagenized background to confirm that they were solely responsible for the altered sensitivity of T3SS-mediated secretion to MBX 2359. Prior to assembly into the T3SS needle, intracellular PscF is complexed with a chaperone, PscG, and a cochaperone, PscE, to maintain PscF in its monomeric form in the bacterial cytoplasm (39). Therefore, we generated *pscEFG* minioperons containing *pscF* from each of the resistant mutant strains, inserted them into the extrachromosomal replicating plasmid pUCP24GW-lacI^{Q}PO (Table 1), and introduced them by electroporation into a *P. aeruginosa* strain (MDM1838) (Table 1) carrying a markerless, in-frame deletion of *pscF* and an integrated ExoS-BLA reporter gene. Sequencing of each complementing plasmid insert confirmed that the *pscF* gene mutations identified previously as SNPs were the only mutations present in the *pscEFG* fragments. The mutant MBX 2359-resistant phenotype was transferred along with the *pscF* allele in each *pscEFG* minioperon, confirming that the mutant *pscF* alleles are necessary and sufficient to provide T3SS secretion that is resistant to MBX 2359 (Table 3 and Fig. 4). Furthermore, the mutant *pscF* alleles provided resistance to four diverse analogs (Fig. 1) of phenoxyacetamide inhibitors that exhibit approximately equal potency against T3SS by cells carrying wild-type *pscF* (Table 3 and Fig. 4). These include the original screening hit MBX 1641 as well as three analogs with significant alterations in the linker region of the scaffold, MBX 2164, MBX 2614, and MBX 2727. These results confirm that specific mutations in the *pscF* gene render *P. aeruginosa* resistant to phenoxyacetamide-mediated inhibition of type III secretion.

To assess the effects of *pscF* mutations on T3SS-mediated translocation of effectors into mammalian cells in the presence of MBX 2359, a cell culture model was used. The complemented Δ*pscF* strains, which secrete ExoS-BLA fusion protein, were incubated with cultured J774 macrophage cells either alone or with various concentrations of phenoxyacetamide inhibitor. Translocation was quantified by using the fluorescent substrate CCF2-AM, which shifts its fluorescence from green to blue upon cleavage of the cephalosporin linker by a β-lactamase (40). Thus, injection of ExoS-BLA into J774 cells was quantified by measuring the ratio of blue to green fluorescence from J774 cells following incubation with the complemented Δ*pscF* strains. Similar to secretion, ExoS-BLA translocation into J774 cells was resistant to MBX 2359 inhibition when mutant *pscF* alleles were expressed (Table 3 and Fig. 5). These results confirm that specific mutations in the *pscF* gene render *P. aeruginosa* resistant to phenoxyacetamide-mediated inhibition of the injection of T3SS effector proteins.

Mutant *pscF* alleles do not provide resistance of T3SS-mediated secretion to inhibitors with different chemical scaffolds. Several other chemical classes of inhibitors of *P. aeruginosa* T3SS have been described (14, 15, 35). We wished to determine whether the *pscF* mutations conferred protection against a broad range of T3SS inhibitors or whether they were specific for the phenoxyacetamide series. Therefore, we examined the potency of a diverse set of inhibitors against T3SS-mediated secretion of the ExoS-BLA reporter fusion protein by the same Δ*pscF* strains carrying each of

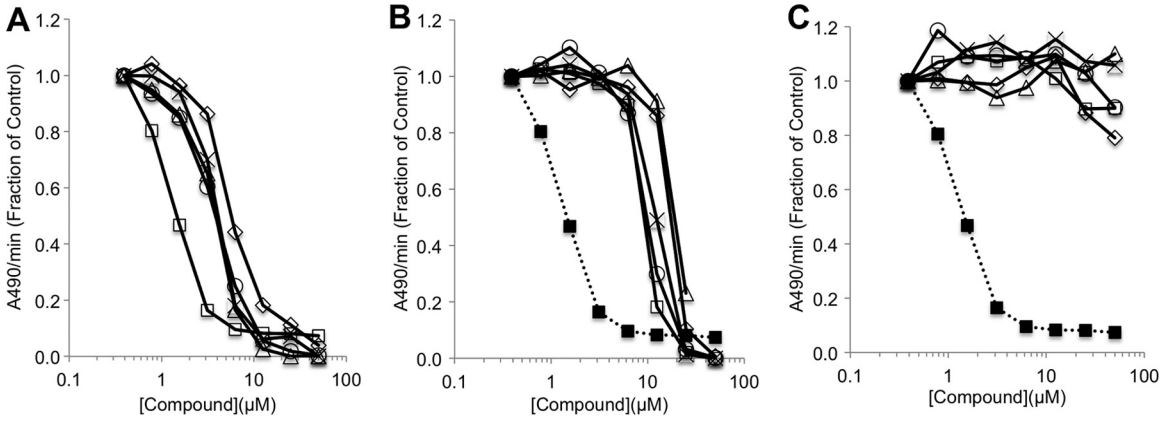

FIG 4 Mutant *pscF* alleles provide T3SS secretion resistance to five phenoxyacetamide analogs. The original screening hit, MBX 1641 (◇), and analogs MBX 2359 (□), MBX 2164 (△), MBX 2614 (○), and MBX 2727 (✖) were tested for inhibition of T3SS-mediated secretion of ExoS-BLA carried out by Δ*pscF* PAO1 cells complemented with *lac*-promoted *pscEFG* on extrachromosomal plasmid pUCP24. The strains and *pscF* alleles were wild-type MDM1912 (A), MDM1967 [PscF(V62I)] (B), and MDM1886 [PscF(R75H)] (C). For reference, the MBX 2359 concentration response versus the wild-type *pscF* allele from panel A is shown in panels B and C as a dotted line.

the four mutant *pscF* alleles on pUCP24. T3SS-mediated secretion of ExoS-BLA by cells carrying each of the four mutant *pscF* alleles was not cross-resistant to inhibitors with nonphenoxyacetamide scaffolds (Table 3 and Fig. 6), including an acylated hydrazone (35), a phenylmaleimide (15), and a thiazoloindole (14) (Fig. 1). These results suggest that these other scaffolds do not interact with PscF or that they interact with a different region of the PscF protein.

Residues capable of conferring inhibitor resistance are in close proximity in a T3SS needle homology model. Full-length isolated T3SS needle proteins are not amenable to crystal structure studies because of their tendency to form needles *in vitro* spontaneously; however, truncated versions and cocrystal structures with chaperoned forms of PscF and its *Yersinia* homolog YscF have been solved (41–43). These structures indicate that the three amino acid residues capable of conferring resistance to the phenoxyacetamide inhibitors are not close enough to form a small-molecule binding site in the relatively rigid alpha-helical C-terminal portion of monomeric PscF complexed with its chaperones, PscE and PscG. In addition, a binding site mapping calculation also failed to identify any small-molecule binding sites in this heterotrimeric structure (B. Li, unpublished data). Hence, we reasoned that this soluble intracellular form of PscF does not interact with the inhibitors. Structural models for the assembled T3SS needle have been proposed for two needle proteins with significant homology to PscF, the *Salmonella* T3SS protein PrgI, based on cryoelectron microscopy and solid-state NMR data (36, 44), and the *Shigella* MxiH, based on X-ray data of the truncated monomer and cryoelectron microscopy (43, 45). Recent immunoelectron microscopy studies indicate that the N-terminal region of the needle protein is on the outer surface of assembled PrgI and MxiH needles (36, 44), and we used the corresponding model of assembled PrgI (36) to estimate the structure of PscF in a T3SS needle (Fig. 7A and B). In this homology model, the 85-residue PscF adopts a rigid conformation comprising four structural elements: an N-terminal extended domain (residues 1 to 11), an α-helix (α1) (residues 12 to 39), a loop (residues 40 to 48), and a C-terminal α-helix (α2) (residues 49 to 85). The PscF subunits form a

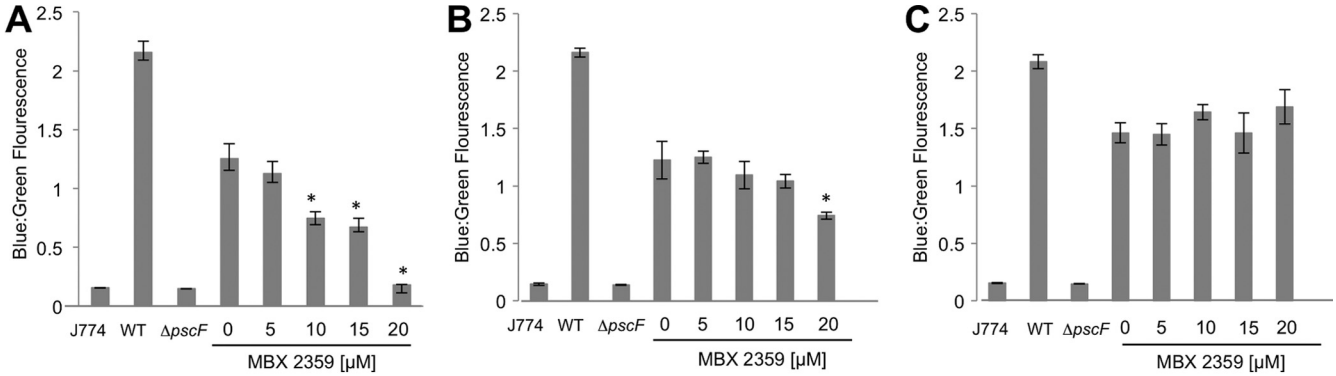

FIG 5 Mutant *pscF* alleles provide T3SS translocation resistance to phenoxyacetamide MBX 2359. Inhibitor or diluent (dimethylsulfoxide) was tested at the indicated concentration for inhibition of T3SS-mediated translocation detected by the β-lactamase-sensitive fluorescent substrate CCF2-AM and carried out by Δ*pscF P. aeruginosa* PAO1 cells complemented with *lac*-promoted *pscEFG* on extrachromosomal plasmid pUCP24. The strains and *pscF* alleles were wild-type MDM1912 (A), MDM1967 [PscF(V62I)] (B), and MDM1886 [PscF(R75H)] (C). The J774 bar indicates the addition of CCF2-AM to J774 cells in the absence of bacteria. The WT and Δ*pscF* bars indicate the addition of CCF2-AM to J774 cells infected with wild-type *P. aeruginosa* and with uncomplemented Δ*pscF P. aeruginosa*, respectively. *, $P < 0.005$ by two-tailed paired Student *t* test.

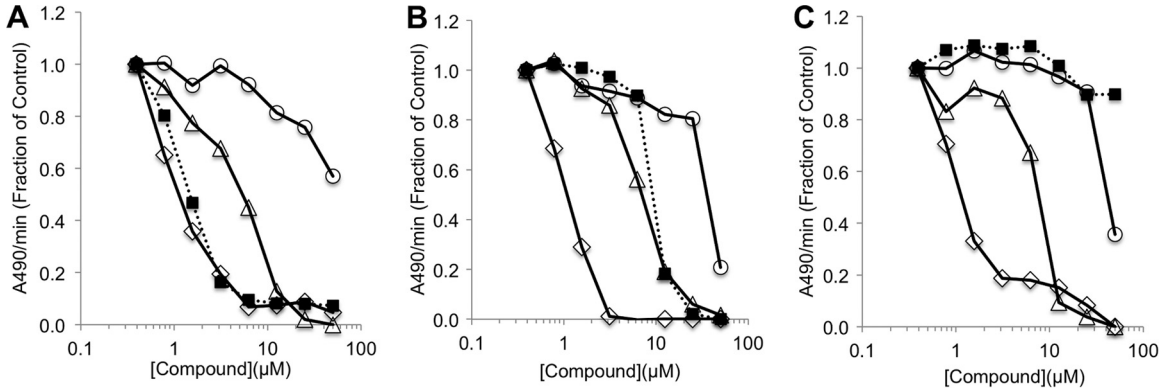

FIG 6 Mutant *pscF* alleles fail to provide T3SS secretion resistance to three nonphenoxyacetamide inhibitors. The sensitivity of secretion to a concentration dilution series of T3SS inhibitors INP0007 (◇), CBG-5376648 (△), CBG-6594330 (○), and the phenoxyacetamide MBX 2359 (■) is shown versus Δ*pscF* PAO1 cells complemented with *lac*-promoted *pscEFG* on extrachromosomal plasmid pUCP24. The strains and *pscF* alleles were wild-type MDM1912 (A), MDM1967 [PscF(V62I)] (B), and MDM1886 [PscF(R75H)] (C).

right-handed helical assembly with roughly 11 subunits per two turns. The extended amino-terminal domain of each PscF subunit is positioned on the surface of the needle, and the α-helical carboxy-terminal domain of each PscF (α2 helix) subunit is positioned inside the needle. Intersubunit interactions are formed by hydrophobic helix-helix packing, while the C-terminal α2 helix hydrophilic residues, which are highly conserved, form the hydrophilic lumen of the needle (36). In this model, the three amino acid residues, which are capable of conferring resistance to phenoxyacetamides when altered, exhibit the following properties: (i) all three appear sufficiently close to one another in the α2 domains of the polymerized form to participate in a single phenoxyacetamide binding site (Fig. 7C and D), (ii) each of the three residues is provided by a different PscF subunit (Fig. 7CD), and (iii) two of the three (R75 and G80) face the lumen of the needle, while the third (V62) is close to and behind R75 (Fig. 7B). These findings suggest that the phenoxyacetamide inhibitors bind to the assembled PscF needle and that they may block T3SS function by affect-

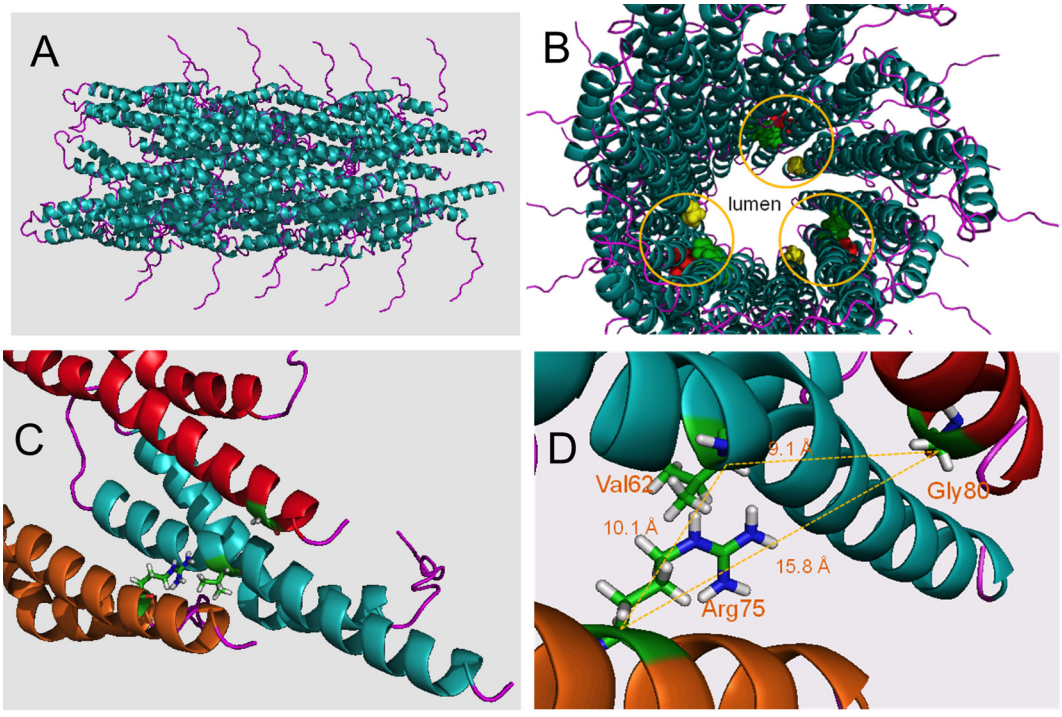

FIG 7 Comparative homology model of the *P. aeruginosa* T3SS needle complex. Ribbon representations show different subunits. (A) Side view. (B) Top view with residues Val62 (red), Arg75 (green), and Gly80 (yellow) shown in space-filling format for three different putative inhibitor interaction sites (circled). Loops joining α helices are shown in purple, as are extended chains positioned on the surface of the needle complex representing the N-terminal domains. Cyan helices represent the α1 and α2 helical structures. Closeup view of three PscF subunits shown in ribbon format, with residues Val62, Arg75, and Gly80 highlighted in stick format (C) and with inter-α-carbon distances shown (D). Each residue is in a different PscF subunit, and the alpha-helical ribbons are colored differently to represent the three different subunits.

ing subunit-subunit interactions to inhibit needle assembly or stability or by binding in, and altering the hydrophilicity of, the needle lumen to inhibit function.

DISCUSSION

The results of this study suggest a new vulnerable molecular target in the complex *P. aeruginosa* T3SS apparatus, the needle protein PscF. Use of the highly potent and selective phenoxyacetamide inhibitor series to select mutations in *pscF* conferring resistance implicates both the PscF needle protein and the specific small-molecule inhibitor as a useful receptor-ligand pair for the potential development of therapeutics or prophylactics. Indeed, the T3SS is one of the most validated virulence targets for drug development based on a wealth of animal infection model and human association studies as well as ongoing clinical studies of the anti-PcrV monoclonal antibody KB001 (19, 20). Prior to this report, PcrV was the only validated structural protein target for intervention in T3SS. This new discovery of a putative second vulnerable T3SS component, the PscF needle protein, may increase the feasibility of discovering useful inhibitors of T3SS. Inhibition of PscF may block T3SS at a more proximal stage in the secretion/translocation process than does inhibition of PcrV, and the use of combinations of inhibitors of both targets may provide synergy and reduce the development of resistance. Furthermore, the fact that both PcrV and the putative target PscF are extracellular eliminates the possibility of resistance to small-molecule inhibitors by efflux, a frequent cause of antibiotic resistance in *P. aeruginosa*.

In principle, it is possible that PscF is not the direct target of the phenoxyacetamide inhibitors and that the observed alterations in PscF transmit conformational changes to a different protein target, which is the actual site of interaction with phenoxyacetamides. However, this seems unlikely for three reasons. First, mutations capable of generating inhibitor-resistant T3SS were not found in other genes despite mutagenesis and selection sufficient to identify four independent *pscF* mutants, each of which is capable of generating an inhibitor-resistant T3SS apparatus. Second, all three of the amino acid residues critical for MBX 2359-mediated inhibition of T3SS appear to be in close enough proximity in structural models of polymerized PscF to interact with an inhibitor of the size of the phenoxyacetamides. Third, even a conservative substitution of His for Arg75, which is arguably less likely to produce conformational changes in PscF, provides over 100-fold resistance to phenoxyacetamide inhibitors without affecting T3SS function detectably. Therefore, our results strongly support the idea that the multimeric form of PscF is the target of the phenoxyacetamide T3SS inhibitors. Although the precise mechanism of action of the inhibitors is not yet clear, biochemical studies are under way to confirm the target and define the mechanism of action of the inhibitors.

The inhibitor specificity of the resistance provided by the *pscF* mutant alleles is quite striking. All four *pscF* mutant alleles provided resistance only to the phenoxyacetamide series of inhibitors, including a range of varied phenoxyacetamides. We have not examined all of the >300 analogs available, but it seems possible that analogs exhibit a range of potencies against the mutants depending on precisely how they interact with the binding site. Such data may help probe the nature of the binding site. The potency of three other chemotypes of published *P. aeruginosa* T3SS inhibitors was not affected by the mutant *pscF* alleles. While these other classes of T3SS inhibitors may interact with PscF at one or more sites distinct from the phenoxyacetamide site, it is also possible that they target other proteins and can be used to define additional inhibitor vulnerabilities in T3SS. For this reason, we have initiated studies utilizing the same selection strain and scheme to identify mutations providing resistance to these other scaffolds. It is not yet possible to predict whether these selections will yield useful mutants, as the success of the selection using the phenoxyacetamide scaffold was at least in part due to the exquisite specificity of this compound series for T3SS inhibition. The approach of converting the T3SS virulence factor into an essential function through the linkage between secretory activity and transcription may be transferrable to other bacterial species, such as those of *Yersinia*, which have a T3SS that is evolutionarily close to that of *P. aeruginosa* and which preserve the function/transcription linkage.

The success in isolating mutations providing resistance to a T3SS inhibitor raises the question of whether resistance will emerge in clinical use of optimized versions of these inhibitors. First, it is important to note that spontaneous inhibitor resistance-conferring mutations did not arise at a particularly high frequency. Initially, the spontaneous mutant selection process was overwhelmed by apparent transcriptional regulatory mutants, possibly in regulatory elements encoded by *exsA*, *exsD*, or *exsCEB*, among others (1). These mutants answered the selection by inducing expression of the gentamicin resistance gene *aacC1* from the *exoT* promoter in the presence of MBX 2359 as well as in the absence of EGTA (which allowed us to eliminate them rapidly from further analysis) but did not provide T3SS secretion that was truly resistant to MBX 2359, as measured in the nitrocefin-based ExoS-BLA assay. Therefore, we used a chemical mutagen to increase the odds of obtaining target mutants. While this approach was effective, it precludes direct measurement of the spontaneous target mutation frequency. However, rough estimates suggest that the spontaneous frequency of true inhibitor-resistant mutants is $\leq 10^{-9}$. Another unknown is the strength of selection for resistance in the context of clinical use. Since T3SS plays an important role in establishing and disseminating infection, it seems likely that some selection pressure will be exerted *in vivo*. Three factors mitigate this concern to some degree: (i) since T3SS inhibitors do not kill *P. aeruginosa* cells directly, the selective pressure is expected to be less than that from an antibiotic; (ii) drugs derived from these T3SS inhibitors would be used clinically, at least initially, in combination with an antipseudomonal antibiotic, likely providing some synergy and reducing development of resistance to either component; and (iii) resistance to T3SS inhibitors may confer a fitness cost. In fact, we plan to evaluate the existing mutants for virulence in animal models of infection.

In summary, the phenoxyacetamide series of T3SS inhibitors implicate a new target in the complex T3SS nanomachine that is susceptible to inhibition by small molecules. The highly responsive SAR, including exquisite stereoselectivity, of these inhibitors indicates a very specific interaction with PscF. These properties, together with the absence of a human PscF homolog, suggest that this class of compounds may be optimized to produce a novel antivirulence factor drug. Such drugs will likely be used in combination with antipseudomonal antibiotics to inhibit the T3SS-mediated intoxication of phagocytes and thereby potentiate a robust host innate immune response and enhance the antibacterial activity of the coadministered antibiotics. Given the propensity of *P. aeruginosa* to develop resistance to conventional antibiotics, such novel therapies are urgently needed.

ACKNOWLEDGMENTS

We thank Stephen Lory (Harvard Medical School) and Timothy Opperman (Microbiotix) for helpful discussions and suggestions. We thank Ming Di and Debra Mills for assistance in plasmid and strain construction and in assaying inhibitor potency. We thank Heather Howell, Greg Tyson, Stephanie Rangel, and Egon Ozer for assistance with the immunoblotting and translocation assays and the whole-genome sequence analysis.

This project was supported by award numbers AI068185 and AI099269 (to D.T.M.) and award numbers AI075191 and AI053674 (to A.R.H.) by the National Institute of Allergy and Infectious Disease of the National Institutes of Health. The content is solely the responsibility of the authors and does not necessarily represent the official views of the National Institutes of Health. The funders had no role in study design, data collection and analysis, decision to publish, or preparation of the manuscript.

REFERENCES

1. **Hauser AR.** 2009. The type III secretion system of Pseudomonas aeruginosa: infection by injection. Nat. Rev. Microbiol. **7:**654–665. http://dx.doi.org/10.1038/nrmicro2199.
2. **Izore T, Job V, Dessen A.** 2011. Biogenesis, regulation, and targeting of the type III secretion system. Structure **19:**603–612. http://dx.doi.org/10.1016/j.str.2011.03.015.
3. **Engel J, Balachandran P.** 2009. Role of Pseudomonas aeruginosa type III effectors in disease. Curr. Opin. Microbiol. **12:**61–66. http://dx.doi.org/10.1016/j.mib.2008.12.007.
4. **Coburn B, Sekirov I, Finlay BB.** 2007. Type III secretion systems and disease. Clin. Microbiol. Rev. **20:**535–549. http://dx.doi.org/10.1128/CMR.00013-07.
5. **Shaver CM, Hauser AR.** 2004. Relative contributions of Pseudomonas aeruginosa ExoU, ExoS, and ExoT to virulence in the lung. Infect. Immun. **72:**6969–6977. http://dx.doi.org/10.1128/IAI.72.12.6969-6977.2004.
6. **Smith RS, Wolfgang MC, Lory S.** 2004. An adenylate cyclase-controlled signaling network regulates Pseudomonas aeruginosa virulence in a mouse model of acute pneumonia. Infect. Immun. **72:**1677–1684. http://dx.doi.org/10.1128/IAI.72.3.1677-1684.2004.
7. **El Solh AA, Akinnusi ME, Wiener-Kronish JP, Lynch SV, Pineda LA, Szarpa K.** 2008. Persistent infection with Pseudomonas aeruginosa in ventilator-associated pneumonia. Am. J. Respir. Crit. Care Med. **178:**513–519. http://dx.doi.org/10.1164/rccm.200802-239OC.
8. **El-Solh AA, Hattemer A, Hauser AR, Alhajhusain A, Vora H.** 2012. Clinical outcomes of type III Pseudomonas aeruginosa bacteremia. Crit. Care Med. **40:**1157–1163. http://dx.doi.org/10.1097/CCM.0b013e3182377906.
9. **Hauser AR, Cobb E, Bodi M, Mariscal D, Valles J, Engel JN, Rello J.** 2002. Type III protein secretion is associated with poor clinical outcomes in patients with ventilator-associated pneumonia caused by Pseudomonas aeruginosa. Crit. Care Med. **30:**521–528. http://dx.doi.org/10.1097/00003246-200203000-00005.
10. **Roy-Burman A, Savel RH, Racine S, Swanson BL, Revadigar NS, Fujimoto J, Sawa T, Frank DW, Wiener-Kronish JP.** 2001. Type III protein secretion is associated with death in lower respiratory and systemic Pseudomonas aeruginosa infections. J. Infect. Dis. **183:**1767–1774. http://dx.doi.org/10.1086/320737.
11. **Zhuo H, Yang K, Lynch SV, Dotson RH, Glidden DV, Singh G, Webb WR, Elicker BM, Garcia O, Brown R, Sawa Y, Misset B, Wiener-Kronish JP.** 2008. Increased mortality of ventilated patients with endotracheal Pseudomonas aeruginosa without clinical signs of infection. Crit. Care Med. **36:**2495–2503. http://dx.doi.org/10.1097/CCM.0b013e318183f3f8.
12. **Negrea A, Bjur E, Ygberg SE, Elofsson M, Wolf-Watz H, Rhen M.** 2007. Salicylidene acylhydrazides that affect type III protein secretion in Salmonella enterica serovar Typhimurium. Antimicrob. Agents Chemother. **51:**2867–2876. http://dx.doi.org/10.1128/AAC.00223-07.
13. **Kauppi AM, Nordfelth R, Uvell H, Wolf-Watz H, Elofsson M.** 2003. Targeting bacterial virulence: inhibitors of type III secretion in Yersinia. Chem. Biol. **10:**241–249. http://dx.doi.org/10.1016/S1074-5521(03)00046-2.
14. **Harmon DE, Davis AJ, Castillo C, Mecsas J.** 2010. Identification and characterization of small-molecule inhibitors of Yop translocation in Yersinia pseudotuberculosis. Antimicrob. Agents Chemother. **54:**3241–3254. http://dx.doi.org/10.1128/AAC.00364-10.
15. **Aiello D, Williams JD, Majgier-Baranowska H, Patel I, Peet NP, Huang J, Lory S, Bowlin TL, Moir DT.** 2010. Discovery and characterization of inhibitors of Pseudomonas aeruginosa type III secretion. Antimicrob. Agents Chemother. **54:**1988–1999. http://dx.doi.org/10.1128/AAC.01598-09.
16. **Grier MC, Garrity-Ryan LK, Bartlett VJ, Klausner KA, Donovan PJ, Dudley C, Alekshun MN, Tanaka SK, Draper MP, Levy SB, Kim OK.** 2010. N-hydroxybenzimidazole inhibitors of ExsA MAR transcription factor in Pseudomonas aeruginosa: in vitro anti-virulence activity and metabolic stability. Bioorg. Med. Chem. Lett. **20:**3380–3383. http://dx.doi.org/10.1016/j.bmcl.2010.04.014.
17. **Baer M, Sawa T, Flynn P, Luehrsen K, Martinez D, Wiener-Kronish JP, Yarranton G, Bebbington C.** 2009. An engineered human antibody fab fragment specific for Pseudomonas aeruginosa PcrV antigen has potent antibacterial activity. Infect. Immun. **77:**1083–1090. http://dx.doi.org/10.1128/IAI.00815-08.
18. **Frank DW, Vallis A, Wiener-Kronish JP, Roy-Burman A, Spack EG, Mullaney BP, Megdoud M, Marks JD, Fritz R, Sawa T.** 2002. Generation and characterization of a protective monoclonal antibody to Pseudomonas aeruginosa PcrV. J. Infect. Dis. **186:**64–73. http://dx.doi.org/10.1086/341069.
19. **Francois B, Luyt CE, Dugard A, Wolff M, Diehl JL, Jaber S, Forel JM, Garot D, Kipnis E, Mebazaa A, Misset B, Andremont A, Ploy MC, Jacobs A, Yarranton G, Pearce T, Fagon JY, Chastre J.** 2012. Safety and pharmacokinetics of an anti-PcrV PEGylated monoclonal antibody fragment in mechanically ventilated patients colonized with Pseudomonas aeruginosa: a randomized, double-blind, placebo-controlled trial. Crit. Care Med. **40:**2320–2326. http://dx.doi.org/10.1097/CCM.0b013e31825334f6.
20. **Milla CE, Chmiel JF, Accurso FJ, Vandevanter DR, Konstan MW, Yarranton G, Geller DE, KB001 Study Group.** 2013. Anti-PcrV antibody in cystic fibrosis: a novel approach targeting Pseudomonas aeruginosa airway infection. Pediatr. Pulmonol. doi:http://dx.doi.org/10.1002/ppul.22890.
21. **Sato H, Hunt ML, Weiner JJ, Hansen AT, Frank DW.** 2011. Modified needle-tip PcrV proteins reveal distinct phenotypes relevant to the control of type III secretion and intoxication by Pseudomonas aeruginosa. PLoS One **6:**e18356. http://dx.doi.org/10.1371/journal.pone.0018356.
22. **Holloway BW, Krishnapillai V, Morgan AF.** 1979. Chromosomal genetics of Pseudomonas. Microbiol. Rev. **43:**73–102.
23. **Bradley DE.** 1974. The adsorption of Pseudomonas aeruginosa pilus-dependent bacteriophages to a host mutant with nonretractile pili. Virology **58:**149–163. http://dx.doi.org/10.1016/0042-6822(74)90150-0.
24. **de Lorenzo V, Timmis KN.** 1994. Analysis and construction of stable phenotypes in gram-negative bacteria with Tn5- and Tn10-derived mini-transposons. Methods Enzymol. **235:**386–405. http://dx.doi.org/10.1016/0076-6879(94)35157-0.
25. **Stover CK, Pham XQ, Erwin AL, Mizoguchi SD, Warrener P, Hickey MJ, Brinkman FS, Hufnagle WO, Kowalik DJ, Lagrou M, Garber RL, Goltry L, Tolentino E, Westbrock-Wadman S, Yuan Y, Brody LL, Coulter SN, Folger KR, Kas A, Larbig K, Lim R, Smith K, Spencer D, Wong GK, Wu Z, Paulsen IT, Reizer J, Saier MH, Hancock RE, Lory S, Olson MV.** 2000. Complete genome sequence of Pseudomonas aeruginosa PAO1, an opportunistic pathogen. Nature **406:**959–964. http://dx.doi.org/10.1038/35023079.
26. **Chuanchuen R, Murata T, Gotoh N, Schweizer HP.** 2005. Substrate-dependent utilization of OprM or OpmH by the Pseudomonas aeruginosa MexJK efflux pump. Antimicrob. Agents Chemother. **49:**2133–2136. http://dx.doi.org/10.1128/AAC.49.5.2133-2136.2005.
27. **Moir DT, Di M, Moore RA, Schweizer HP, Woods DE.** 2008. Cellular reporter screens for inhibitors of Burkholderia pseudomallei targets in Pseudomonas aeruginosa. Trans. R. Soc. Trop. Med. Hyg. **102**(Suppl 1)**:**S152–S162. http://dx.doi.org/10.1016/S0035-9203(08)70033-6.
28. **Hoang TT, Kutchma AJ, Becher A, Schweizer HP.** 2000. Integration-proficient plasmids for Pseudomonas aeruginosa: site-specific integration and use for engineering of reporter and expression strains. Plasmid **43:**59–72. http://dx.doi.org/10.1006/plas.1999.1441.
29. **Diaz MH, Hauser AR.** 2010. Pseudomonas aeruginosa cytotoxin ExoU is injected into phagocytic cells during acute pneumonia. Infect. Immun. **78:**1447–1456. http://dx.doi.org/10.1128/IAI.01134-09.
30. **Roehl RA, Phibbs PV, Jr.** 1982. Characterization and genetic mapping of fructose phosphotransferase mutations in Pseudomonas aeruginosa. J. Bacteriol. **149:**897–905.
31. **Wolfgang MC, Lee VT, Gilmore ME, Lory S.** 2003. Coordinate regula-

tion of bacterial virulence genes by a novel adenylate cyclase-dependent signaling pathway. Dev. Cell **4:**253–263. http://dx.doi.org/10.1016/S1534-5807(03)00019-4.

32. **Moir DT, Di M, Opperman T, Schweizer HP, Bowlin TL.** 2007. A high-throughput, homogeneous, bioluminescent assay for Pseudomonas aeruginosa gyrase inhibitors and other DNA-damaging agents. J. Biomol. Screen. **12:**855–864. http://dx.doi.org/10.1177/1087057107304729.
33. **Choi KH, Kumar A, Schweizer HP.** 2006. A 10-min method for preparation of highly electrocompetent Pseudomonas aeruginosa cells: application for DNA fragment transfer between chromosomes and plasmid transformation. J. Microbiol. Methods **64:**391–397. http://dx.doi.org/10.1016/j.mimet.2005.06.001.
34. **Hauser AR, Kang PJ, Engel JN.** 1998. PepA, a secreted protein of Pseudomonas aeruginosa, is necessary for cytotoxicity and virulence. Mol. Microbiol. **27:**807–818. http://dx.doi.org/10.1046/j.1365-2958.1998.00727.x.
35. **Nordfelth R, Kauppi AM, Norberg HA, Wolf-Watz H, Elofsson M.** 2005. Small-molecule inhibitors specifically targeting type III secretion. Infect. Immun. **73:**3104–3114. http://dx.doi.org/10.1128/IAI.73.5.3104-3114.2005.
36. **Loquet A, Sgourakis NG, Gupta R, Giller K, Riedel D, Goosmann C, Griesinger C, Kolbe M, Baker D, Becker S, Lange A.** 2012. Atomic model of the type III secretion system needle. Nature **486:**276–279. http://dx.doi.org/10.1038/nature11079.
37. **Rietsch A, Vallet-Gely I, Dove SL, Mekalanos JJ.** 2005. ExsE, a secreted regulator of type III secretion genes in Pseudomonas aeruginosa. Proc. Natl. Acad. Sci. U. S. A. **102:**8006–8011. http://dx.doi.org/10.1073/pnas.0503005102.
38. **Urbanowski ML, Lykken GL, Yahr TL.** 2005. A secreted regulatory protein couples transcription to the secretory activity of the Pseudomonas aeruginosa type III secretion system. Proc. Natl. Acad. Sci. U. S. A. **102:**9930–9935. http://dx.doi.org/10.1073/pnas.0504405102.
39. **Quinaud M, Chabert J, Faudry E, Neumann E, Lemaire D, Pastor A, Elsen S, Dessen A, Attree I.** 2005. The PscE-PscF-PscG complex controls type III secretion needle biogenesis in Pseudomonas aeruginosa. J. Biol. Chem. **280:**36293–36300. http://dx.doi.org/10.1074/jbc.M508089200.
40. **Zlokarnik G, Negulescu PA, Knapp TE, Mere L, Burres N, Feng L, Whitney M, Roemer K, Tsien RY.** 1998. Quantitation of transcription and clonal selection of single living cells with beta-lactamase as reporter. Science **279:**84–88. http://dx.doi.org/10.1126/science.279.5347.84.
41. **Quinaud M, Ple S, Job V, Contreras-Martel C, Simorre JP, Attree I, Dessen A.** 2007. Structure of the heterotrimeric complex that regulates type III secretion needle formation. Proc. Natl. Acad. Sci. U. S. A. **104:**7803–7808. http://dx.doi.org/10.1073/pnas.0610098104.
42. **Sun P, Tropea JE, Austin BP, Cherry S, Waugh DS.** 2008. Structural characterization of the Yersinia pestis type III secretion system needle protein YscF in complex with its heterodimeric chaperone YscE/YscG. J. Mol. Biol. **377:**819–830. http://dx.doi.org/10.1016/j.jmb.2007.12.067.
43. **Deane JE, Roversi P, Cordes FS, Johnson S, Kenjale R, Daniell S, Booy F, Picking WD, Picking WL, Blocker AJ, Lea SM.** 2006. Molecular model of a type III secretion system needle: implications for host-cell sensing. Proc. Natl. Acad. Sci. U. S. A. **103:**12529–12533. http://dx.doi.org/10.1073/pnas.0602689103.
44. **Demers JP, Sgourakis NG, Gupta R, Loquet A, Giller K, Riedel D, Laube B, Kolbe M, Baker D, Becker S, Lange A.** 2013. The common structural architecture of Shigella flexneri and Salmonella typhimurium type three secretion needles. PLoS Pathog. **9:**e1003245. http://dx.doi.org/10.1371/journal.ppat.1003245.
45. **Fujii T, Cheung M, Blanco A, Kato T, Blocker AJ, Namba K.** 2012. Structure of a type III secretion needle at 7-A resolution provides insights into its assembly and signaling mechanisms. Proc. Natl. Acad. Sci. U. S. A. **109:**4461–4466. http://dx.doi.org/10.1073/pnas.1116126109.